

Reprocessable Polymer Networks Containing Sulfur-Based, Percolated Dynamic Covalent Cross-Links and Percolated or Non-Percolated, Static Cross-Links

Logan M. Fenimore, Mohammed A. Bin Rusayyis, Claire C. Onsager, Matthew A. Grayson, and John M. Torkelson*

One method to improve the properties of covalent adaptable networks (CANs) is to reinforce them with a fraction of permanent cross-links without sacrificing their (re)processability. Here, a simple method to synthesize poly(n-hexyl methacrylate) (PHMA) and poly(n-lauryl methacrylate) (PLMA) networks containing static dialkyl disulfide cross-links (utilizing bis(2-methacryloyl)oxyethyl disulfide, or DSDMA, as a permanent cross-linker) and dynamic dialkylamino sulfur-sulfur cross-links (utilizing BITEMPS methacrylate as a dissociative dynamic covalent cross-linker) is presented. The robustness and (re)processability of the CANs are demonstrated, including the full recovery of cross-link density after recycling. The authors also investigate the effect of static cross-link content on the stress relaxation responses of the CANs with and without percolated, static cross-links. As PHMA and PLMA have very different activation energies of their respective cooperative segmental mobilities, it is shown that the dissociative CANs without percolated, static cross-links have activation energies of stress relaxation that are dominated by the dissociation of BiTEMPS methacrylate cross-links rather than by the cooperative relaxations of backbone segments, i.e., the alpha relaxation. In CANs with percolated, static cross-links, the segmental relaxation of side chains, i.e., the beta relaxation, is critical in allowing for large-scale stress relaxation and governs their activation energies of stress relaxation.

1. Introduction

Conventional polymer networks, known as thermosets, cannot be recycled into high-value products because permanent cross-links make it challenging to reprocess and recycle them in the melt state. [1-5] This means that spent polymer networks cannot be easily transformed into new products, leading to sustainability losses from the disposal of the material and economic losses due to the high value of the original network materials. However, dynamic covalent polymer networks,[3] also known as covalent adaptable networks^[6,7] (CANs), offer a potential solution to the sustainability and economic problems of unrecyclable polymer networks. CANs possess tremendous utility in that they are designed to allow for structural rearrangement at processing conditions through dynamic covalent chemistries, making them reprocessable. Through reversible reactions triggered by an external stimulus, dynamic covalent cross-links can be broken down and re-formed or exchanged, allowing the network material (which would otherwise be unprocessable) to be reprocessed and reused for high-value applications. Although reversible polymer networks using

L. M. Fenimore, J. M. Torkelson Department of Chemical and Biological Engineering Northwestern University Evanston, IL 60208, USA E-mail: j-torkelson@northwestern.edu

The ORCID identification number(s) for the author(s) of this article can be found under https://doi.org/10.1002/marc.202400303

© 2024 The Author(s). Macromolecular Rapid Communications published by Wiley-VCH GmbH. This is an open access article under the terms of the Creative Commons Attribution-NonCommercial License, which permits use, distribution and reproduction in any medium, provided the original work is properly cited and is not used for commercial purposes.

DOI: 10.1002/marc.202400303

M. A. Bin Rusayyis, J. M. Torkelson
Department of Materials Science and Engineering
Northwestern University
Evanston, IL 60208, USA
C. C. Onsager, M. A. Grayson
Department of Electrical and Computer Engineering
Northwestern University
Evanston, IL 60208, USA



the Diels–Alder reaction as the dynamic covalent chemistry were first studied decades ago,^[8,9] it is only in recent years that various dynamic covalent chemistries have been employed in research on reprocessable polymer networks.^[4,10–23] This has led to significant progress in the field and the development of new materials that may be recycled and reused, reducing waste and increasing polymer sustainability.

CANs may be classified based on their type(s) of dynamic covalent chemistry. Dissociative dynamic covalent chemistries involve linkages breaking in response to an external stimulus such as elevated temperature (T) and reforming upon the removal of the stimulus. The Diels-Alder reaction[9,13,24-28] and alkoxyamine dynamic bonds^[2,29–34] are examples of dissociative dynamic covalent chemistries. When a CAN with dissociative linkages is subjected to sufficiently high temperatures, it may transform into a combination of branched and linear chains via dissociative reactions, allowing it to be reprocessed. Dynamic covalent cross-links then re-form upon cooling. On the other hand, associative dynamic covalent chemistries involve the simultaneous breaking and forming of bonds (and, thus, theoretically maintaining a constant number of cross-links) to enable rearrangement of the network structure during reprocessing. Associative-type dynamic covalent chemistries include reactions such as transesterification^[23,35,36] or transamination.^[20,37,38] CANs based strictly on associative dynamic covalent chemistries are also known as vitrimers. [4,39] Some CANs exhibit two or more dynamic covalent chemistries as well as both dissociative and associative dynamic covalent chemistries.[40-44]

While the dynamic covalent chemistries characteristic of CANs have led to the development of polymer networks that may be recycled and reused, these networks containing dynamic covalent cross-links often fail to emulate the properties of thermosets fully or to meet the requirements of conventional thermoset applications.[45] As one example, due to the dynamic nature of their cross-links at elevated temperatures, CANs often exhibit poor creep resistance at elevated temperatures [15,20,22,34,36,39,46–48] where creep is defined as a continuous, time-dependent deformation under a constant load or stress.[15,20,22,34,36,39,46-49] On the contrary, conventional thermosets contain permanent crosslinks, imbuing them with excellent creep resistance. [50-52] Several methods have been investigated to improve the properties of reprocessable CANs to be more similar to those of their thermoset counterparts.[4,11,15,22,33,34,36,42,46,48,53-74] One method that has shown promise was reported in 2018 by Torkelson and coworkers[36] as well as Sumerlin and coworkers[54] and involves incorporating a fraction of permanent cross-links into CANs without precluding their reprocessability. Other groups have since used similar approaches. [55,56] Through careful CAN design and control of the ratio of static to dynamic covalent cross-links within the network, it is possible to improve the robustness of CANs significantly while still allowing for their full reprocessability.[36]

Static cross-links may also be utilized to regulate the dynamics and topological rearrangement of CANs.^[45] In 2010, Matyjaszewski and coworkers reported the synthesis of polymer networks containing trithiocarbonate-based dynamic covalent cross-links that undergo exchange reactions via an addition-fragmentation mechanism.^[75] They found that, by introducing a portion of static cross-links to the networks, it becomes pos-

sible to adjust their swelling characteristics while maintaining the same overall cross-link density. More dynamic covalent cross-links led to greater adaptation and rearrangement of the gels in response to their chemical environment. This enabled some of the mechanical stress caused by solvent diffusion within the polymer networks to be relieved, leading to networks with higher swelling ratios. Precise control of the topology of CANs achieved through static cross-links may also lead to materials with superior self-healing properties. [45,76]

Indeed, the effects of static cross-links on the dynamics and topological rearrangements of CANs are critical not only to their swelling characteristics and self-healing capabilities but also to their processability, and these effects may be probed further through investigations of stress relaxation and corresponding apparent Arrhenius activation energies. Given that the incorporation of static cross-links into CANs is a promising avenue to meet the performance requirements for some applications of conventional thermosets, it is important to study the viscoelastic properties of CANs as this will provide a better understanding of their thermomechanical responses as well as their processability.

For the first time and by exclusively free-radical methods, we synthesized polymer networks containing two kinds of sulfur-based cross-linkers in which one cross-linker contained dialkyl disulfide static bonds and the other cross-linker contained dialkylamino sulfur-sulfur dynamic covalent bonds (See Figure 1) Dialkyl disulfide bonds have relatively high bond dissociation energies (250-300 kJ mol⁻¹),^[77] and, in the absence of catalysts, act as static cross-links.[78-81] Dialkylamino sulfur-sulfur bonds have much lower bond dissociation energies (110-130 kJ mol⁻¹)[79,82,83] and are dynamic even in the absence of a catalyst. [15,17,81,84-88] Thus, the CANs reported in this study, which are synthesized via free-radical copolymerizations of the cross-linkers with n-hexyl methacrylate or n-lauryl methacrylate, contain both sulfur-based static and dynamic covalent cross-links. We demonstrate that the fraction of static cross-links in the CANs may be tuned to improve their hightemperature thermomechanical properties. We also demonstrate the (re)processability of the synthesized CANs containing both static and dynamic covalent cross-links, including property recovery associated with cross-link density after recycling. Thus, the robust thermomechanical properties of the CANs are not at the expense of their (re)processability. We further examine the effect of static cross-links on the responses and underlying mechanisms of stress relaxation of the dual networks containing dynamic and static cross-links.

2. Results and Discussion

We synthesized two poly(*n*-hexyl methacrylate) (PHMA) covalent adaptable networks (CANs), abbreviated PHMA-B4-D1 and PHMA-B3-D2, and four poly(*n*-lauryl methacrylate) (PLMA, also known as poly(*n*-dodecyl methacrylate)) CANs, abbreviated PLMA-B5, PLMA-B4-D1, PLMA-B3-D2, and PLMA-B2-D3. We made the CANs with two cross-linkers: BiTEMPS methacrylate (B), a dynamic covalent cross-linker containing dialkylamino sulfur-sulfur bonds that we reported in previous studies (Figure 1),^[15,17,86,89,90] and bis(2-methacryloyl)oxyethyl disulfide (DSDMA or D), a commercially available dialkyl disulfide cross-linker (Figure 1) that, in the absence of catalyst, incorporates

15213927, Downloaded from https://onlinelibrary.wiley.com/doi/10.1002/marc.202400303 by Readcube (Labiva Inc.), Wiley Online Library on [170702024]. See the Terms and Conditions (https://onlinelbrary.wiley.com/terms-and-conditions) on Wiley Online Library for rules of use; OA articles are governed by the applicable Creative Commons License

www.advancedsciencenews.com



$$n$$
-Hexyl methacrylate (HMA)

 n -Lauryl methacrylate (LMA)

 n -Lauryl methacrylate (LMA)

PHMA CAN or PLMA CAN

Figure 1. Synthesis of poly(n-hexyl methacrylate) (PHMA) CANs and poly(n-lauryl methacrylate) (PLMA) CANs via free-radical copolymerizations of n-hexyl methacrylate or n-lauryl methacrylate with BiTEMPS methacrylate (B) and DSDMA (D) at 70 °C for 24 h using AIBN as initiator.

static cross-links into the percolated network.[78-81] In the CAN abbreviations PHMA-Bx-Dy and PLMA-Bx-Dy, x and y represent the mol% of BiTEMPS methacrylate and DSDMA utilized in the CAN synthesis, respectively. As an example, we made the PHMA-B3-D2 network with 3.0 mol% BiTEMPS methacrylate and 2.0 mol% DSDMA. In these CANs, which were prepared via freeradical copolymerizations at 70 °C using 1.0 mol% azobisisobutyronitrile (AIBN) as initiator, we fixed the total combination of the static and dynamic covalent cross-links at 5.0 mol% while the ratios of the dynamic to static cross-links (mol mol⁻¹) were varied. Thus, we may study the viscoelastic and thermomechanical properties of the CANs as the levels of static and dynamic covalent cross-links are changed. We did not synthesize a PHMA-B5 sample (containing 5 mol% BiTEMPS methacrylate and no DSDMA) as we have studied PHMA CANs containing 5 mol% BiTEMPS methacrylate extensively in previous reports; [15,17,86,89,90] our success in synthesizing robust and reprocessable CANs using BiTEMPS methacrylate in previous studies in part motivates this study. It is worth noting that the polymerizing vinyl moieties

in the two cross-linkers, BiTEMPS methacrylate and DSDMA, are both methacrylates and, hence, the two cross-linkers should have similar reactivity with the monomers, *n*-hexyl methacrylate (HMA) and *n*-lauryl methacrylate (LMA). In addition, given that the polymerizing moieties in the two cross-linkers are similar to the polymerizing moiety in the base monomers, all or nearly all of the cross-linkers added in the polymerization mixtures would be expected to incorporate into the synthesized networks.

Our synthesized CANs were insoluble in toluene and had high gel contents (> 90%; Table S1, Supporting Information), confirming the highly cross-linked nature of the networks. We also characterized the CANs by differential scanning calorimetry (DSC). PHMA-B4-D1 and PHMA-B3-D2 exhibited glass transition temperatures ($T_{\rm g}$ values) of 14 °C and 11 °C, respectively (Figure S1a, Supporting Information). The $T_{\rm g}$ values of the PLMA CANs could not be discerned via DSC (Figure S1b, Supporting Information) due to their being obscured by the broad melting transition characteristic of n-lauryl side chains, which are long enough to crystallize at very low temperatures. [92] Peak melting temperatures



www.mrc-journal.de

Table 1. Glass transition and melting point temperatures and crystallinity of CANs (by DSC).

CAN ^{a)}	$T_{g,midpoint} [^{\circ}C]^{b)}$	T _{m,peak} [°C] ^{c)}	Crystallinity [%] ^{c)}	
PHMA-B4-D1	14	_	0	
PHMA-B3-D2	11	_	0	
PLMA-B5	_	-38	8	
PLMA-B4-D1	_	-42	3	
PLMA-B3-D2	_	-41	4	
PLMA-B2-D3	_	-38	3	

a) CANs are named using the following convention: PHMA-Bx-Dy or PLMA-Bx-Dy, where x and y represent the mol% of BiTEMPS methacrylate (B) and DSDMA (D) utilized in the CAN synthesis, respectively; $^{b)}T_{g}$ information was not observed by DSC for PLMA CANs due to broad melting transitions; [93] c) PHMA CANs do not exhibit melting transitions.

 $(T_{m,peak}$ values) and crystallinities of the PLMA CANs (Table 1) ranged from −42 °C to −38 °C and from 3% to 8%, respectively, and are in general alignment with previously reported values for neat PLMA. $^{[93,94]}$ There is no trend between $T_{
m m,peak}$ values or crystallinities and the ratio of dynamic to static cross-links in the PLMA CANs. We also investigated the processability of the CANs via compression molding. For the levels and ratios of dynamic to static cross-links considered in this study, the PHMA and PLMA CANs were able to be processed at 130 °C for 1 h to obtain healed, uniform films (Figure S2, Supporting Information).

We also synthesized a permanently cross-linked PHMA network with 5.0 mol% DSDMA and no BiTEMPS methacrylate (PHMA-D5). This polymerization was carried out at the same conditions as the other PHMA and PLMA networks. Considering that PHMA-D5 was synthesized without any catalysts to contain only static cross-links (as the exclusion of BiTEMPS methacrylate in the PHMA-D5 synthesis resulted in no dynamic covalent cross-links in its network structure), it was expected that assynthesized pieces of PHMA-D5 would be unable to be processed into a healed film. We attempted twice to process as-synthesized pieces of PHMA-D5 into a film at 130 °C for 1 h; neither of the attempts was successful. From the compression molding attempts, we obtained crushed, unhealed films that crumbled upon handling (Figure \$3, Supporting Information), a result that precludes further thermomechanical characterization of PHMA-D5. This result also demonstrates the static nature of the dialkyl disulfide cross-links afforded by the DSDMA cross-linker in the absence of catalysts in the PHMA-D5 network and highlights the importance of BiTEMPS methacrylate in providing dynamic covalent cross-links in the CANs that allow for their processability.

We characterized the thermomechanical properties of the 1stmolded PHMA and PLMA CANs by high-temperature (*T*) DMA. As shown in **Figure 2**, the storage modulus (*E*') curves of the network samples exhibit rubbery plateaus well above their T_{σ} values (T > 80 °C), further confirming the cross-linked nature of these networks. See Table 2 for E' values of the PHMA CANs and PLMA CANs at 120 °C. Although the two 1st-molded PHMA CANs contain different ratios of dynamic to static cross-links, they exhibit similar E' values in their rubbery plateaus (0.97 \pm 0.12 MPa for PHMA-B4-D1 and 0.97 \pm 0.24 MPa for PHMA-B3-D2 at 120 °C), which can be taken as a measure of their cross-link densities according to Flory's ideal rubber elasticity theory.^[95]

These results indicate that the two networks contain similar total concentrations of cross-linkers. This is also confirmed by the tan δ results as both PHMA-B4-D1 and PHMA-B3-D2 networks exhibit a tan δ peak T at ~37 °C (Figure 2b). In addition, the PHMA CANs possess greater cross-link densities than the PLMA CANs, except for PLMA-B3-D2 (the PLMA CAN with the highest cross-link density), as evidenced by their *E'* rubbery plateaus of greater magnitude than most of those of the PLMA CANs. Thus, longer polymethacrylate side chain lengths generally lead to lower cross-link densities in resulting polymethacrylate CANs, a result mostly irrespective of their ratios of dynamic to static cross-links.

Unlike the PHMA CANs, the PLMA CANs do not all exhibit similar E' values in their rubbery plateaus. PLMA-B5 and PLMA-B4-D1 exhibit overlapping E' rubbery plateaus within experimental uncertainty (0.47 \pm 0.06 MPa and 0.49 \pm 0.04 MPa at 120 °C, respectively); PLMA-B2-D3 and PLMA-B3-D2 exhibit successively larger E' rubbery plateaus (0.70 \pm 0.06 MPa and 0.87 \pm 0.05 MPa at 120 °C, respectively). Thus, in the PLMA CANs, there is no direct relationship between static cross-link content and cross-link density; yet, in general, CANs with larger amounts of static cross-links (PLMA-B3-D2 and PLMA-B2-D3) exhibit larger cross-link densities than CANs with smaller amounts of static cross-links (PLMA-B5 and PLMA-B4-D1). This observation is different from that observed in PHMA CANs in this study. Interestingly, PHMA-B4-D1 and PHMA-B3-D2, which contain some static cross-links, possess E'rubbery plateaus of lower magnitude than those previously reported for PHMA CANs synthesized with 5 mol% BiTEMPS methacrylate and, therefore, containing only dynamic covalent cross-links (such CANs would be abbreviated PHMA-B5 in this study). [15,17] Thus, the effect of static cross-link incorporation into polymethacrylate CANs on cross-link density is unclear. This point as well as our observation that PLMA CANs of the same total cross-linker loading (5 mol%) exhibit different cross-link densities merit further investigation.

As *T* increases above 200 °C, the *E'* values of PHMA-B4-D1, PLMA-B5, PLMA-B4-D1, and PLMA-B3-D2 decrease gradually, indicating losses in the cross-link density at these conditions. When T reaches ~220 °C, the networks lose their integrity and undergo terminal flow. Given that the dynamic covalent cross-linker BiTEMPS methacrylate has a decomposition $T(T_d)$ 5% weight loss temperature) of 202 °C,[85] this flow may be associated with or aided by the degradation of these dynamic cross-links. Different behaviors are observed for PHMA-B3-D2 and PLMA-B2-D3. For these CANs, E' decreases gradually when the sample is heated above 200 °C. However, the CANs exhibit a secondary plateau above 220 °C, suggesting the percolation of the static cross-links in these CANs. PHMA-B3-D2 exhibits this short plateau up to ~238 °C, above which its E' decreases until the sample flows at ~275 °C. PLMA-B2-D3 sustains this plateau up to 275 °C without reaching terminal flow. This secondary plateau is attributed to the larger amount of static dialkyl disulfide cross-links in these networks. Given the higher bond dissociation energy of dialkyl disulfide bonds and the absence of catalysts, higher temperatures are required to make the dissociation of dialkyl disulfide bonds apparent. (We note that DSDMA exhibited a $T_{
m d}$ value of 182 °C (Figure S4, Supporting Information) Thus, while the terminal flow of PHMA-B3-D2 may be aided by the degradation of DSDMA and

15213927, 0, Downloaded from https://onlinelibrary.wiley.com/doi/10.1002/marc.202400303 by Readcube (Labtiva Inc.), Wiley Online Library on [17/07/2024]. See the Terms

and-conditions) on Wiley Online Library for rules of use; OA articles are governed by the applicable Creative Commons License

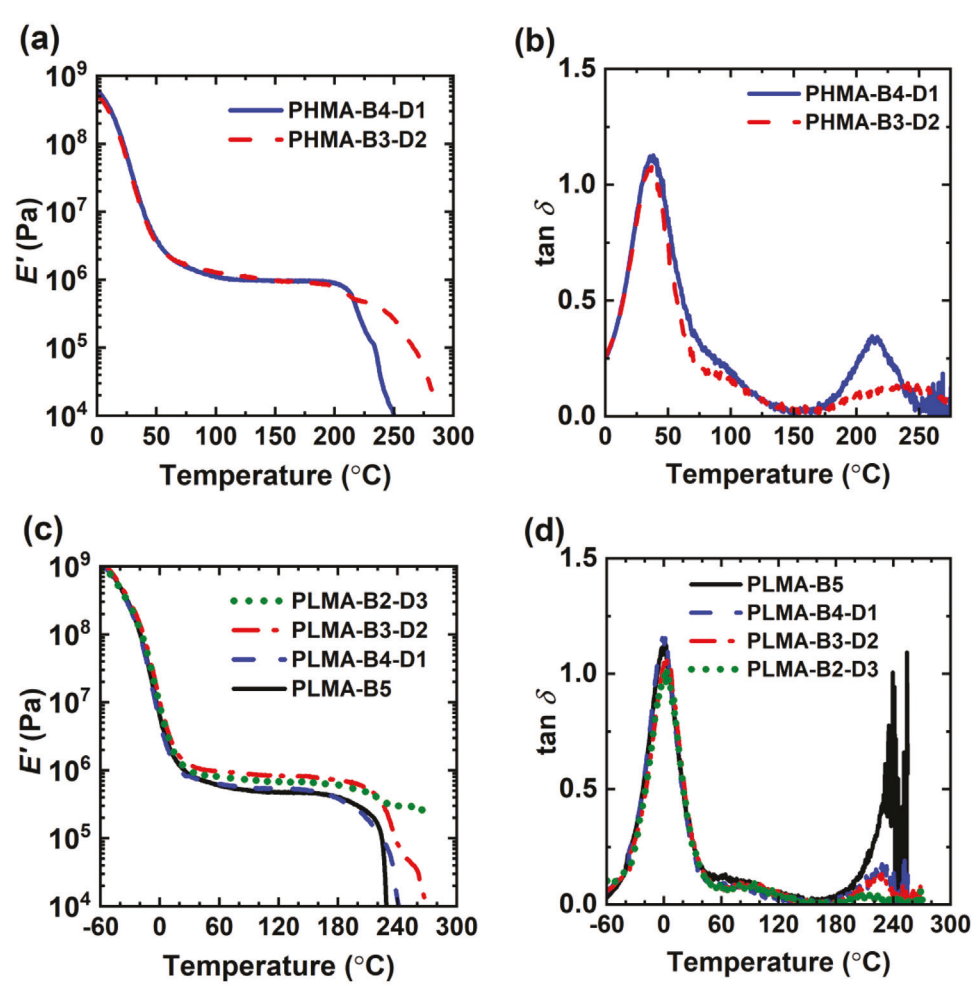


Figure 2. Tensile storage modulus (E') and damping ratio (tan $\delta = E''/E'$) as functions of temperature for 1st-molded (a/b) PHMA CANs and (c/d) PLMA CANs.

BiTEMPS methacrylate, the difference in terminal flow behavior between PHMA-B3-D2 and the other PHMA and PLMA CANs besides PLMA-B2-D3 is likely attributable to the higher content of the static cross-links in PHMA-B3-D2.) Our results indicate that incorporating static cross-links into dynamic networks can enhance the thermal stability of these networked materials.

To investigate the recyclability of the CANs, we cut the 1stmolded films into small pieces and compression-molded them at 130 °C for 1 h to obtain 2nd-molded films. Recyclability was evaluated using swelling tests in toluene and dynamicmechanical analysis (DMA) characterization and by comparing the properties of the recycled (i.e., 2nd mold) samples to those of their 1st-molded predecessors. Table S1, Supporting Information gives the gel contents of the successively molded CANs. We observed that the PHMA CANs reproduced their gel contents within experimental uncertainty with reprocessing. Figure 3 shows that the E' curves of the 2nd-molded samples of PHMA-B4-D1 and PHMA-B3-D2 display a rubbery plateau, further indicating that cross-linked networks were obtained after reprocessing. In addition, over the T range of 0 °C to 150 °C, the tan δ curves of the molded networks each show a unimodal single peak, suggesting a complete homogenization of the network samples. No-

Table 2. Thermomechanical properties of PHMA CANs and PLMA CANs via DMA as a function of molding step.

CAN ^{a)}	Mold	E' (at 120 °C) [MPa]	Tan δ peak T [°C]
PHMA-B4-D1	1st mold	0.97 ± 0.12	37 ± 3
	2nd mold	0.92 ± 0.09	39 ± 6
PHMA-B3-D2	1st mold	0.97 ± 0.24	38 ± 1
	2nd mold	0.87 ± 0.09	36 ± 2
PLMA-B5	1st mold	0.47 ± 0.06	0 ± 1
	2nd mold	0.43 ± 0.07	0 ± 1
PLMA-B4-D1	1st mold	0.49 ± 0.04	0 ± 1
	2nd mold	0.53 ± 0.01	0 ± 2
PLMA-B3-D2	1st mold	0.87 ± 0.05	1 ± 2
	2nd mold	0.81 ± 0.02	0 ± 1
PLMA-B2-D3	1st mold	0.70 ± 0.06	1 ± 1
	2nd mold	0.74 ± 0.02	1 ± 2

a) CANs are named using the following convention: PHMA-Bx-Dy or PLMA-Bx-Dy, where x and y represent the mol% BITEMPS methacrylate (B) and the mol% DSDMA (D) used in the CAN synthesis, respectively.

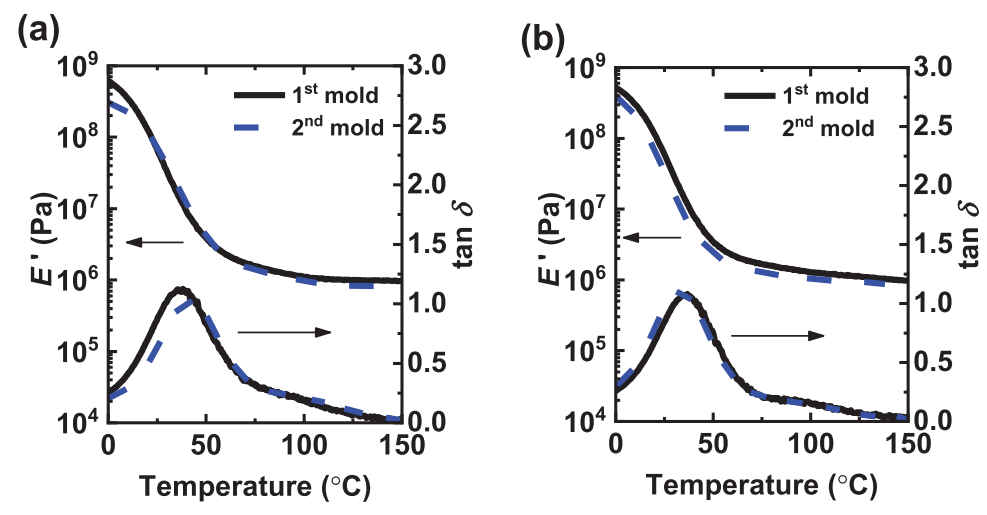


Figure 3. Tensile storage modulus (E') and damping ratio ($\tan \delta$) of a) PHMA-B4-D1 and b) PHMA-B3-D2 networks as functions of molding step and temperature. (We note that these specific curves displayed are each one of several data curves taken for their respective molds. As shown in Table 2, E' values and $\tan \delta$ peak Ts of successive molds of these CANs are within experimental uncertainty of one another.)

tably, the 1st- and 2nd-molded samples of both PHMA-B4-D1 and PHMA-B3-D2 networks exhibit the same *E'* values in the rubbery plateau region with experimental uncertainty (Table 2). These gel content and DMA results indicate that cross-link density and its associated properties are recovered and maintained in PHMA CANs even when static dialkyl disulfide cross-links replaced some dynamic covalent cross-links. Thus, PHMA CANs containing 5 mol% cross-links may contain upward of 40% static cross-links before their reprocessability is affected.

We observed similar results when investigating the recyclability of PLMA CANs. All of our PLMA CANs were able to be reprocessed into healed, 2nd-molded films. As seen in Figure 4 and Table 2, the 2nd-molded PLMA CANs reproduced the E' rubbery plateaus and tan δ curves within experimental uncertainty of their respective 1st-molded CANs, indicating that PLMA CANs fully recovered their cross-link densities with reprocessing like the PHMA CANs. It is worth noting that PLMA-B2-D3 exhibited a sharp decrease in its gel content after being processed into a 1st-molded sample (96 ± 2% gel for as-synthesized sample versus 76 \pm 3% gel for 1st-molded sample). Considering that this phenomenon did not occur in any other PHMA or PLMA CAN, all of which contain less static cross-links than PLMA-B2-D3, this result is likely due to the greater fraction of static cross-links in PLMA-B2-D3 (3 mol%) affecting the processability of the network. Although 1st-molded PLMA-B2-D3 was unable to recover the gel content determined for its as-synthesized predecessor, 1st-molded PLMA-B2-D3 was able to be reprocessed into a 2nd-molded film which recovered the gel content and thermomechanical properties by DMA of its 1st-molded film. Thus, while the initial processability of PLMA CANs containing 5 mol% cross-links may be affected at some level of static cross-links between 40% and 60%, PLMA CANs containing 5 mol% cross-links may contain upward of 60% static cross-links before their reprocessability is affected.

To this end, we characterized the stress relaxation behaviors of the 1st-molded CANs in the *T* range of 120–150 °C. As shown in **Figure 5a**, PHMA-B4-D1 networks exhibit full stress relaxation

at all tested temperatures, a characteristic of CANs with an active dynamic covalent character. Note that stress relaxation experiments are often assumed to reach a zero asymptotic value and are terminated early, but, here, longer experiments were required to identify non-zero asymptotic behavior as evidence of residual, percolated, permanent cross-links. The stress relaxation rate increased with increasing T, consistent with faster dissociation of the dynamic covalent cross-links. Notably, for PHMA-B4-D1, the stress relaxed completely even though the network contains 1 mol% static dialkyl disulfide cross-links. (By contrast, PHMA networks containing only static dialkyl disulfide cross-links and no dynamic covalent cross-links were reported to be incapable of relaxing stress at 140 °C.[84]) These results suggest that no percolated, permanent cross-links were present in PHMA-B4-D1, which is reasonable given that the network contains only 1 mol% DSDMA.

However, for PHMA-B3-D2, which contains a greater concentration of static DSDMA cross-links equaling 2 mol%, only partial stress relaxation is observed in the T range of 120-150 °C (Figure 5b). At very short times, PHMA-B3-D2 exhibits stress relaxation with relaxation rates similar to those of PHMA-B4-D1. From 120 °C to 140 °C, when ~60% of the initial stress has relaxed, the relaxation slows until it plateaus with residual unrelaxed stress of 35-38% of the initial value. As shown in Figure 5b, further stress relaxation is observed when T is increased to 150 °C, and the residual unrelaxed stress decreases to ~25% of the initial stress value. With 2 mol% DSDMA, unrelaxed residual stresses indicate that percolated, permanent dialkyl disulfide cross-links are formed, a result that aligns with our observation from Figure 2a that PHMA-B3-D2 exhibits a second rubbery plateau at very high temperatures, likely due to percolated, permanent cross-links.

As seen in the stress relaxation curves in **Figure 6**, PLMA-B5, PLMA-B4-D1, and PLMA-B3-D2 behave similarly to PHMA-B4-D1 (which contains non-percolated, static cross-links) in that these PLMA CANs relax stress fully. As with the PHMA CANs, relaxation times of PLMA CANs decrease with increasing

15213927, 0, Downloaded from https://onlinelibrary.wiley.com/doi/10.1002/marc.202400303 by Readcube (Labtiva Inc.), Wiley Online Library on [17/07/2024]. See the Terms and Conditions (https://online.com/doi/10.1002/marc.202400303 by Readcube (Labtiva Inc.), Wiley Online Library on [17/07/2024]. See the Terms and Conditions (https://online.com/doi/10.1002/marc.202400303 by Readcube (Labtiva Inc.), Wiley Online Library on [17/07/2024]. See the Terms and Conditions (https://online.com/doi/10.1002/marc.202400303 by Readcube (Labtiva Inc.), Wiley Online Library on [17/07/2024]. See the Terms and Conditions (https://online.com/doi/10.1002/marc.202400303 by Readcube (Labtiva Inc.), Wiley Online Library on [17/07/2024]. See the Terms and Conditions (https://online.com/doi/10.1002/marc.202400303 by Readcube (Labtiva Inc.), Wiley Online Library on [17/07/2024]. See the Terms and Conditions (https://online.com/doi/10.1002/marc.202400303 by Readcube (Labtiva Inc.), Wiley Online Library on [17/07/2024]. See the Terms and Conditions (https://online.com/doi/10.1002/marc.202400303 by Readcube (Labtiva Inc.), Wiley Online Library on [17/07/2024]. See the Terms and Conditions (https://online.com/doi/10.1002/marc.202400303 by Readcube (Labtiva Inc.), Wiley Online Library on [17/07/2024]. See the Terms and Conditions (https://online.com/doi/10.1002/marc.202400303 by Readcube (Labtiva Inc.), Wiley Online Library on [17/07/2024]. See the Terms and Conditions (https://online.com/doi/10.1002/marc.202400303 by Readcube (Labtiva Inc.), Wiley Online Library on [17/07/2024]. See the Terms and Conditions (https://online.com/doi/10.1002/marc.202400303 by Readcube (Labtiva Inc.), Wiley Online Library on [17/07/2024]. See the Terms and Conditions (https://online.com/doi/10.1002/marc.202400303 by Readcube (Labtiva Inc.), Wiley Online Library on [17/07/2024]. See the Terms and Conditions (https://online.com/doi/10.1002/marc.202400300 by Readcube (https://online.com/doi/10.1002/marc.202400300 by Readcube (https://online.com/doi/10.1002/marc.2024

-and-conditions) on Wiley Online Library for rules of use; OA articles are governed by the applicable Creative Commons License

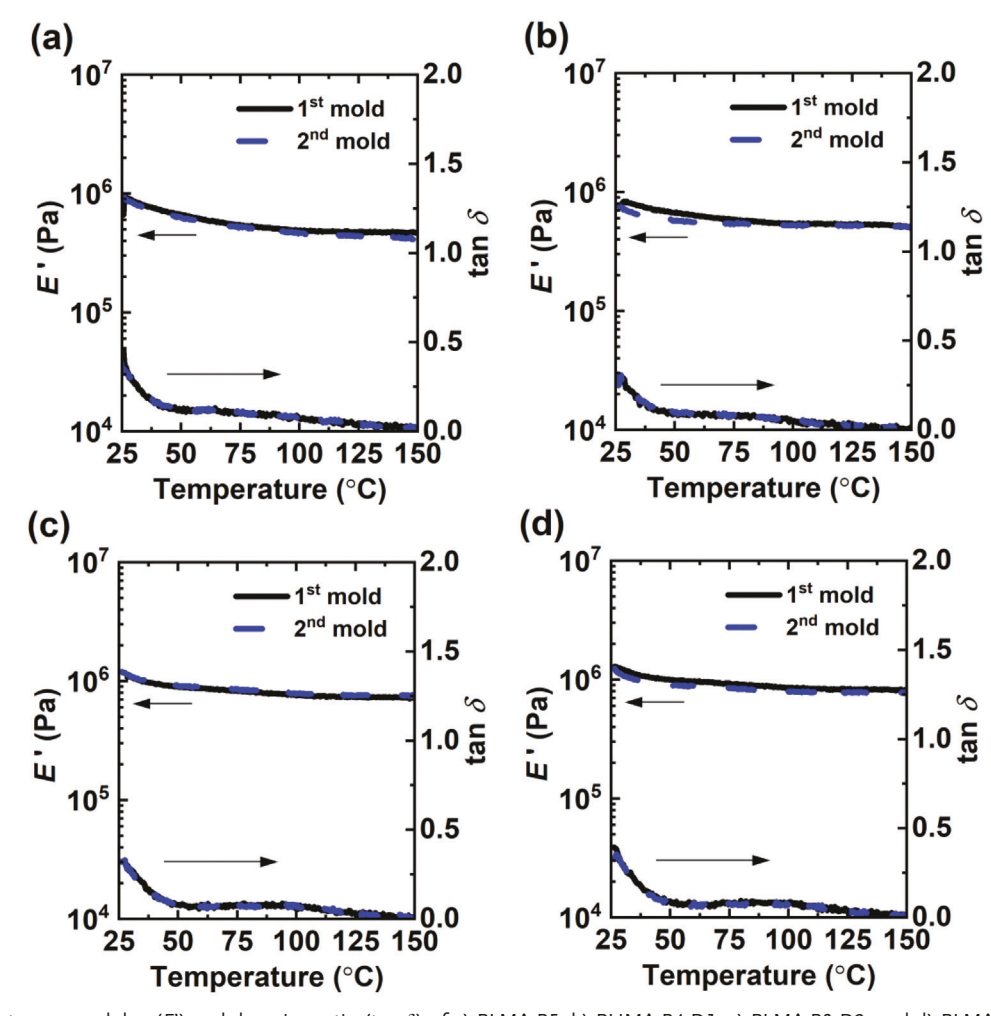


Figure 4. Tensile storage modulus (E') and damping ratio (tan δ) of a) PLMA-B5, b) PHMA-B4-D1, c) PLMA-B3-D2, and d) PLMA-B2-D3 networks as functions of molding step and temperature.

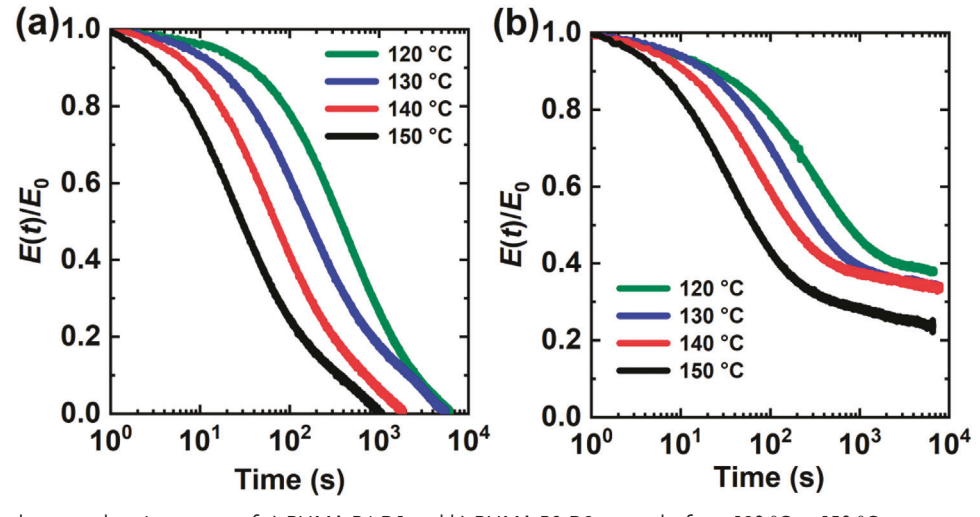


Figure 5. Normalized stress relaxation curves of a) PHMA-B4-D1 and b) PHMA-B3-D2 networks from 120 °C to 150 °C.

15213927, 0, Downloaded from https://onlinelibrary.wiley.com/doi/10.1002/marc.202400303 by Readcube (Labtiva Inc.), Wiley Online Library on [17/07/2024]. See the Terms and Conditions (https:

elibrary.wiley.com/terms-and-conditions) on Wiley Online Library for rules of use; OA articles are governed by the applicable Creative Commons License

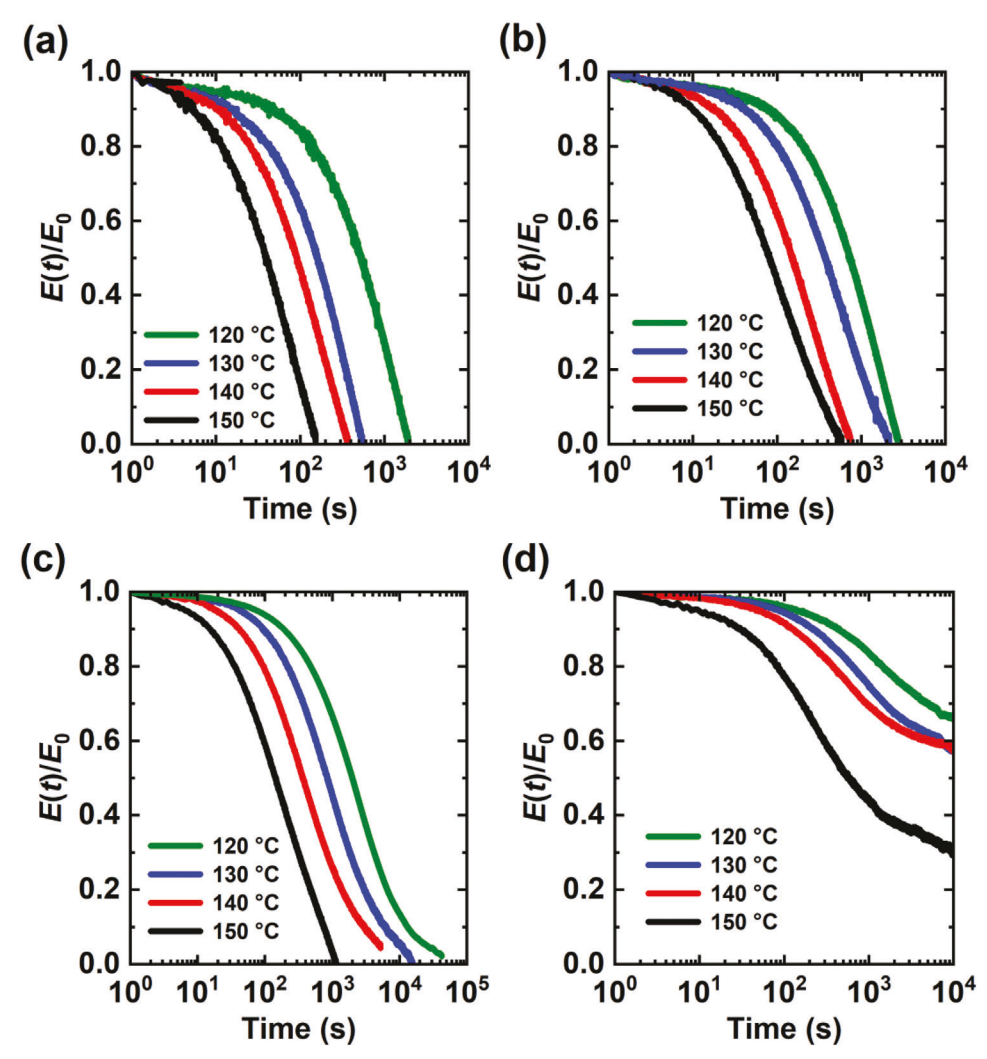


Figure 6. Normalized stress relaxation curves of a) PLMA-B5, b) PLMA-B4-D1, c) PLMA-B3-D2, and d) PLMA-B2-D3 networks from 120 °C to 150 °C.

temperature. Interestingly, relaxation times at each temperature increase from PLMA-B5 to PLMA-B4-D1 to PLMA-B3-D2. Thus, there is an increasing trend between relaxation time and static cross-link content in the PLMA CANs that relax stress fully (despite PLMA-B5 and PLMA-B4-D1 having identical cross-link densities within experimental uncertainty). This observation corroborates our postulate that an increasing presence of static cross-links in the CANs would have a significant impact on their relaxation dynamics, leading to slower relaxations in our cases. It is also worth noting that while PHMA-B3-D2 containing 2 mol% static cross-links is unable to relax stress fully, PLMA-B3-D2, which contains the same amount of static cross-links and possesses the same cross-link density as PHMA-B3-D2 within experimental uncertainty, relaxes stress completely. This may be due to the differences in $T_{\rm g}$ of these two CANs. While $T_{\rm g}$ values cannot be discerned for the PLMA CANs by DSC, we can use the T at which tan δ is a maximum as a proxy for T_{σ} when comparing these networks (the peak T in a tan δ function of T is sometimes referred to as a "shifted" $T_{\rm g}$ value). [15,96] The 1st-molded PLMA-B3-D2 has a tan δ peak T of 1 ± 2 °C, and the 1st-molded PHMA-B3-D2 has a tan δ peak T of 38 \pm 1 °C. Therefore, it can be inferred that a greater than 30 °C difference in $T_{\rm g}$ exists between these CANs, meaning that the tested stress relaxation temperatures of 120–150 °C are further above the $T_{\rm g}$ of PLMA-B3-D2 than they are above that of PHMA-B3-D2. PLMA-B3-D2 being further along in its rubbery plateau at the tested stress relaxation temperatures than PHMA-B3-D2 may have a nonnegligible impact on its relaxation dynamics compared to PHMA-B3-D2, causing it to relax more stress than PHMA-B3-D2 with the same static cross-link content and cross-link density. Future work on this point may be warranted.

Contrary to the other PLMA CANs, PLMA-B2-D3, which contains 3 mol% static cross-links, is unable to relax stress fully in the tested T range (Figure 6d). The curves at 120–140 °C begin to plateau at long times with residual unrelaxed stress between 58%–65% of their initial values. Additional stress relaxation is observed at 150 °C, leaving \sim 32% residual unrelaxed stress. This is due to the presence of percolated, permanent cross-links, again in line with our observation from Figure 2c that PLMA-B2-D3 exhibits a second rubbery plateau at high temperatures, suggesting



www.mrc-journal.de

percolation of permanent cross-links. PLMA-B2-D3 has greater residual stress at several temperatures than PHMA-B3-D2, a result that is likely owed to the greater fraction of static cross-links in PLMA-B2-D3 compared to PHMA-B3-D2. In addition, it would make sense that a CAN that may only relax $\sim\!1/3$ of its stress at 130 °C (the (re)processing T of PHMA and PLMA CANs) would have difficulty being processed at 130 °C as we observed when processing PLMA-B2-D3 into a 1st-molded film with $\sim\!20\%$ less gel than its as-synthesized counterpart.

We note that, ideally, for a network containing percolated, permanent cross-links, the fraction of the residual stress is expected to be independent of T. However, in the case of PHMA-B3-D2 and PLMA-D2-B3, the percolated, permanent dialkyl disulfide cross-links are not perfectly static but rather have some dynamic character that is extremely slow in the absence of external or internal catalysts, even at high temperatures.^[58,78-80] This is why lower residual stresses are recorded at 150 °C compared to the residual stresses measured at 120-140 °C. That said, the extremely slow dynamic character of dialkyl disulfide cross-links without catalysts is also why PHMA-D5 cannot be processed into a healed film. In contrast to PHMA-D5, we note that the percolated, permanent cross-links in PHMA-B3-D2 and the inability of the network to relax stress fully do not prevent it from being processable at 130 °C. Similar results were reported for polybutadiene vitrimers containing dynamic dioxaborolane cross-links and percolated, permanent cross-links.^[55] Our observation contrast with transesterification-based, step-growth vitrimers, in which the presence of percolated, permanent crosslinks prevented effective reprocessing and significantly reduced cross-link density after recovery.[36] We also note that we have previously reported other dynamic dissociative network systems that can be processed at T values where less than 30% of stress relaxation is observed.^[16] This processability is attributed to the use of elevated compressive pressure during the processing of these networks, which is absent during stress relaxation experiments. These results confirm the important role of pressure on the processability of dynamic or partially dynamic covalent polymer networks. These results also suggest that complete stress relaxation is not required to achieve (re)processability with good property recovery. That said, as previously mentioned, PLMA-B2-D3 had some difficulty being processed into a 1st-molded film from as-synthesized pieces. Therefore, although complete stress relaxation is not required for the (re)processability of CANs containing some percolated, permanent cross-links, too many static cross-links can certainly affect processability negatively.

In general, polymers and dynamic covalent polymer networks exhibit a distribution of stress relaxation modes and can rarely be described by a single exponential decay or single relaxation time, as described by the Maxwell model.^[7,15,16,36,42,55,78,97–99] To account for this distribution in stress relaxation, we fit the stress relaxation data of the CANs to the Kohlrausch–Williams–Watts (KWW) stretched exponential decay function: ^[15,36,42,78,99–103]

$$\frac{\sigma(t)}{\sigma_0} = \frac{\sigma_{\text{perm}}}{\sigma_0} + \left(1 - \frac{\sigma_{\text{perm}}}{\sigma_0}\right) \exp\left[-\left(\frac{t}{\tau^*}\right)^{\beta}\right] \tag{1}$$

where $\sigma(t)/\sigma_0$ is the normalized stress at time t, τ^* is a characteristic relaxation time, and β (0 < $\beta \le 1$) is the exponent that controls the shape of the stretched exponential decay and reflects the

Table 3. KWW function parameters and average relaxation times obtained from best fits to stress relaxation data at various temperatures.

CAN ^{a)}	<i>T</i> [°C]	$\sigma_{ m perm}/\sigma_0$	τ* [s]	β	$<\tau>[s]$	R^2
PHMA-B4-D1 ^{b)}	120	0.0048	667	0.65	904	>0.997
	130	0.0044	340	0.50	691	>0.986
	140	0.0071	135	0.55	228	>0.990
	150	0.0086	58	0.51	111	>0.983
PHMA-B3-D2	120	0.38	348	0.66	465	>0.998
	130	0.35	201	0.64	280	>0.991
	140	0.35	104	0.56	171	>0.970
	150	0.25	57	0.45	144	>0.953
PLMA-B5	120	0	737	1	737	>0.988
	130	0	220	1	220	>0.986
	140	0	127	1	127	>0.993
	150	0	55	1	55	>0.994
PLMA-B4-D1	120	0	1020	1	1020	>0.991
	130	0	481	0.98	487	>0.996
	140	0	223	0.94	230	>0.996
	150	0	129	0.82	143	>0.997
PLMA-B3-D2 ^{b)}	120	0.021	3880	0.77	4540	>0.994
	130	0.023	1400	0.67	1850	>0.993
	140	0.055	565	0.71	709	>0.996
	150	0	274	0.71	344	>0.972
PLMA-B2-D3	120	0.65	1930	0.71	2400	>0.998
	130	0.58	1240	0.65	1690	>0.988
	140	0.59	686	0.66	925	>0.993
	150	0.32	394	0.52	725	>0.982

^{a)} CANs are named using the following convention: PHMA-Bx-Dy or PLMA-Bx-Dy, where x and y represent the mol% of BiTEMPS methacrylate (B) and DSDMA (D) utilized in the CAN synthesis, respectively; ^{b)} Fits for PHMA-B4-D1 and PLMA-B3-D2 were also done assuming $\sigma_{\text{perm}}/\sigma_0=0$ to obtain excellent fits with similar fitting parameters as reported here, consistent with complete stress relaxation and the absence of any percolated, permanent cross-links.

breadth of the relaxation distribution, with $\beta=1$ indicating a single relaxation time. The term $\sigma_{\rm perm}/\sigma_0$ is the fraction of residual stress relative to initial stress that remains unrelaxed as the time approaches infinity. For polymers lacking percolated, permanent cross-links, $\sigma_{\rm perm}/\sigma_0$ is expected to be zero within experimental uncertainty. The average relaxation time, $<\tau>$, can be calculated by [100]

$$\langle \tau \rangle = \frac{\tau^* \Gamma(1/\beta)}{\beta} \tag{2}$$

where $\boldsymbol{\Gamma}$ represents the gamma function.

We applied the KWW function in fitting our stress relaxation data to obtain the parameters shown in **Table 3**. We found that β values generally decrease with increasing temperature in all but one of our CANs, indicating broader relaxation distributions at higher temperatures. This trend, which is attributed to the reduction in the network character and, therefore, increased network heterogeneity at higher temperatures, is similar to what we have observed previously in polymethacrylate CANs containing only BiTEMPS cross-links and polymethacrylate CANs based on dissociative hindered urea bonds.^[15,16] We observe that all of the re-

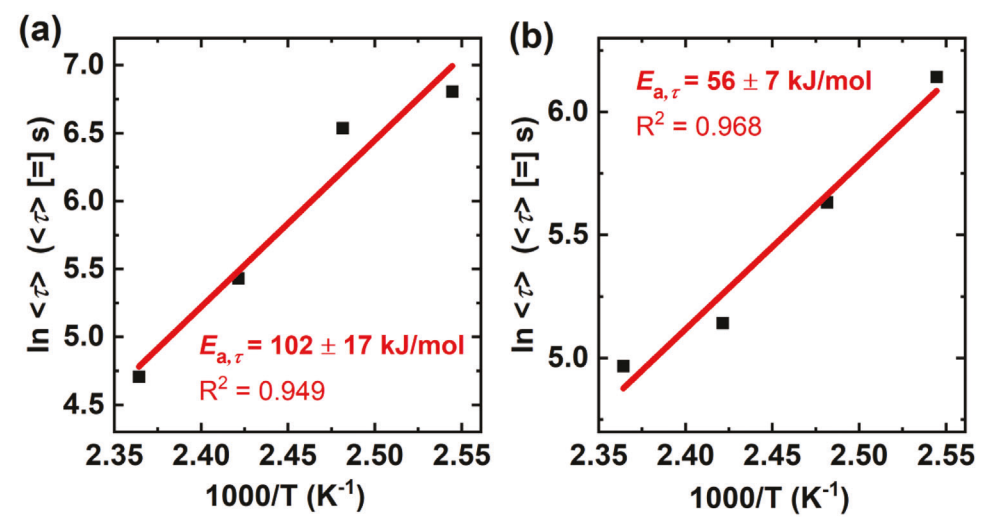


Figure 7. Arrhenius apparent activation energies of stress relaxation for a) PHMA-B4-D1 and b) PHMA-B3-D2 networks via plots of $\ln <\tau >$ as a function of 1000 T^{-1}

laxations of PLMA-B5, the only CAN in this study that is fully dynamic, approximate a single exponential decay (in which β is 1), behavior that is independent of temperature and characteristic of Maxwellian stress relaxation responses.^[104] PLMA-B4-D1, with a cross-link density within experimental uncertainty of PLMA-B5, also exhibits a Maxwellian stress relaxation response at 120 °C.

While stress relaxation being well modeled by a single exponential decay function is rare in polymers and CANs, this phenomenon has been described and encountered previously. Parada and Zhao developed ideal reversible polymer network theory, [105] which predicted that the stress relaxation of dissociative-type CANs without network defects or entanglements may be modeled well by a single exponential decay function; they validated this prediction using reversible hydrogels capable of dynamic covalent phenylboronic acid-diol chemistry. [105] We have also reported dissociative-type CANs exhibiting Maxwellian stress relaxation on two occasions, [86,89] both of which were lightly cross-linked CANs synthesized via freeradical methods. In one of these instances, Fenimore et al. [89] grafted BiTEMPS methacrylate cross-links between the side chains of PHMA to produce lightly cross-linked and entangled CANs that exhibited multimodal stress relaxation; the long-term stress relaxation responses of their CANs approximated a single exponential decay.[89]

We note that PLMA-B5 and PLMA-B4-D1 possess the lowest cross-link densities of the CANs in this study. Based on this information and our previous findings, dissociative-type CANs of low (\lesssim 5 mol%) cross-linker loading resulting in low to moderate cross-link densities likely contain less network defects which ultimately lead to greater network homogeneity and less breadth in stress relaxation distributions. In the case of PLMA-B4-D1, the incorporation of some static cross-links adds heterogeneity to the network which manifests itself as β values being less than 1 at temperatures 130–150 °C. Thus, we conclude that the presence of static cross-links in a CAN will increase its relaxation distribution breadth, other factors such as total cross-linker loading and CAN cross-link density being equal. The use of more controlled polymerization methods could incorporate cross-links more homoge-

neously and offset the increase in relaxation distribution breadth that we observe in the PLMA CANs, with increasing amounts of static cross-links; further study in this regard is warranted.

The average relaxation times of the CANs were found to have approximately Arrhenius temperature dependences (Figures 7 and 8). The apparent activation energies ($E_{a,\tau}$ values) associated with stress relaxation of the CANs in the 120-150 °C temperature range were obtained from the slopes of the linear fits of ln $\langle \tau \rangle$ versus 1000 T^{-1} . The $E_{a,\tau}$ value of PHMA-B4-D1 is 102 \pm 17 kJ mol⁻¹. It is noteworthy that, within experimental uncertainty, this value is equivalent to the bond dissociation energies (BDE) of the disulfide and trisulfide bonds in the BiTEMPS methacrylate cross-links (BDEs = $110-130 \text{ kJ mol}^{-1}$).[79,82-84] Similar outcomes were reported for PHMA CANs containing 5 mol% of BiTEMPS cross-links.[15,89,90] These results suggest that the temperature dependence of the stress relaxation response of PHMA-B4-D1 is dominated by the dissociation of the BiTEMPS methacrylate cross-links instead of being governed by mechanisms such as the diffusion of the cross-links to find new partners with which to reassociate after their initial dissociation. It is also clear that the presence of 1 mol% static dialkyl disulfide cross-links had no apparent effect on the temperature dependence of the network's stress relaxation response relative to previously reported PHMA CANs containing only dynamic covalent cross-links.^[15,90] These results further support the lack of percolated, permanent crosslinks in PHMA-B4-D1.

That said, beyond cross-link chemistry, it is important to understand the role of the CAN backbone in its viscoelastic responses such as stress relaxation. [106] We note that the $E_{\rm a,\tau}$ of PHMA-B4-D1 of $102\pm17\,\rm kJ~mol^{-1}$ as well as previously reported $E_{\rm a,\tau}$ values of PHMA CANs containing BiTEMPS methacrylate cross-links [15,90] are within experimental uncertainty of the effective activation energy ($E_{\rm a,\alpha}^{\rm WLF}$) of cooperative segmental relaxation and monomer friction for PHMA (alpha relaxation) calculated using the Williams–Landel–Ferry (WLF) parameters of PHMA. [107] In the range of tested stress relaxation temperatures in this study (which are well above the $T_{\rm g}$ of PHMA), the $E_{\rm a,\alpha}^{\rm WLF}$ of PHMA is 97–105 kJ mol $^{-1}$. Thus, the cooperative

15213927, 0, Downloaded from https://onlinelibrary.wiley.com/doi/10.1002/marc.202400303 by Readcube (Labtiva Inc.), Wiley Online Library on [17/07/2024]. See the Terms

s-and-conditions) on Wiley Online Library for rules of use; OA articles are governed by the applicable Creative Commons License

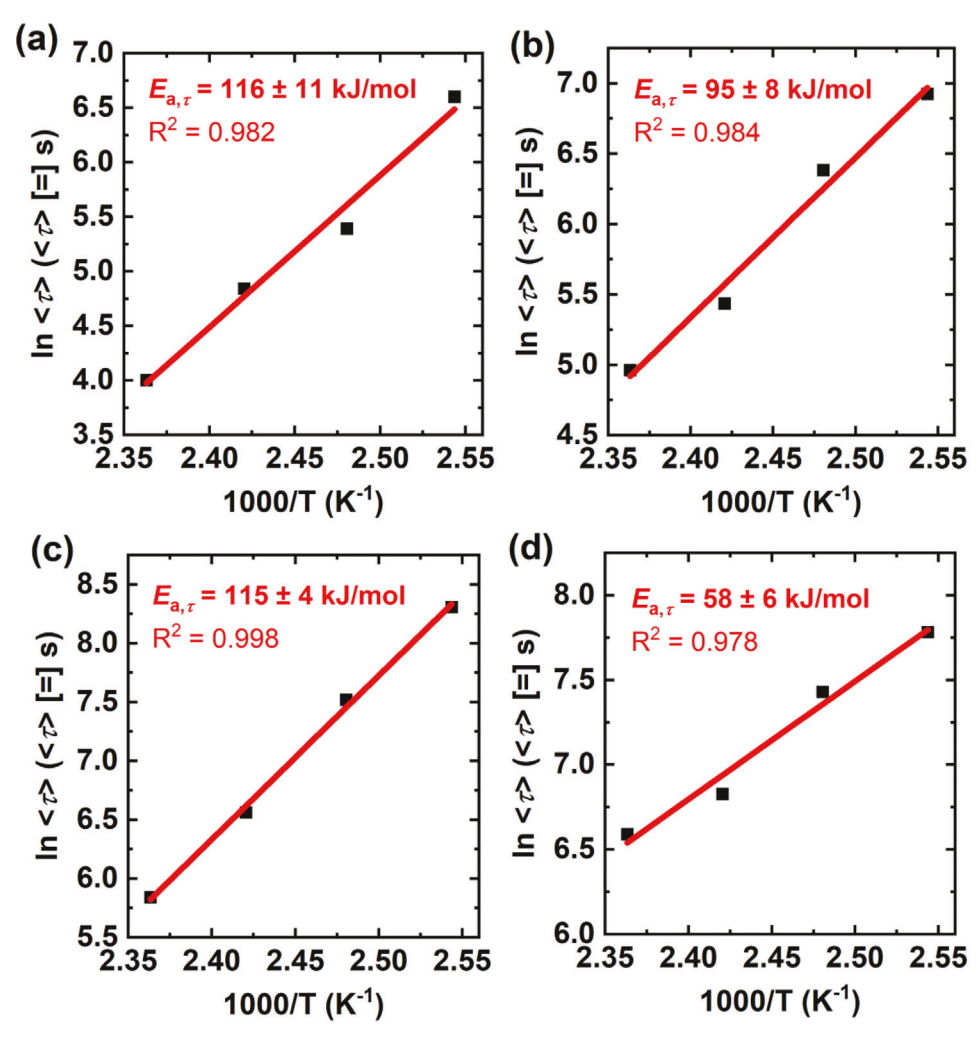


Figure 8. Arrhenius apparent activation energies of stress relaxation for a) PLMA-B5, b) PLMA-B4-D1, c) PLMA-B3-D2, and d) PLMA-B2-D3 networks via plots of $\ln < \tau >$ as a function of 1000 T^{-1} .

segmental relaxation of the PHMA backbone could be the major driving force behind stress relaxation and, therefore, determining the temperature dependence of stress relaxation in our and previously reported PHMA CANs instead of the cross-linker chemistry.

Deconvoluting the mechanisms behind the stress relaxation of PHMA CANs is made more interesting by our results regarding PHMA-B3-D2 in which percolated, permanent cross-links are present in the network architecture. PHMA-B3-D2 exhibits an $E_{\rm a,\tau}$ value of 56 ± 7 kJ mol $^{-1}$. Not only does the presence of some percolated, dialkyl disulfide cross-links affect the relaxation dynamics of the CANs, but also the substantial difference between this $E_{\rm a,\tau}$ and the $E_{\rm a,\tau}$ of PHMA-B4-D1 indicates that this presence leads to a lower temperature dependence of the CAN stress relaxation response, consistent with the static (or significantly less dynamic) nature of these cross-links. Importantly, this $E_{\rm a,\tau}$ of 56 ± 7 kJ mol $^{-1}$ is within experimental uncertainty of the activation energy of the beta relaxation of PHMA ($E_{\rm a,\rho}^{\rm WLF}\sim54$ kJ mol $^{-1}$), which is attributed to the motion of the n-hexyl side chains in PHMA.[107]

We have previously reported PHMA CANs (containing BiTEMPS methacrylate cross-links grafted between *n*-hexyl side chains) having $E_{a,\tau}$ values within experimental uncertainty of the $E_{a,\beta}^{WLF}$ of PHMA.^[89] In those instances, it was logical that the relaxation of n-hexyl side chains, in some cases enabled by dynamic covalent bond dissociation and subsequent exchange, facilitated the motion of backbone chains and, therefore, largescale stress relaxation.^[89,107] As such, we hypothesized that the temperature dependence of stress relaxation of these PHMA CANs with BiTEMPS methacrylate cross-links between n-hexyl side chains resultingly aligned with $E_{a,\beta}^{WLF}$ of PHMA.^[89] It is plausible that an increased presence of static cross-links in PHMA-B3-D2 is shifting the driving force behind stress relaxation to be the relaxation of n-hexyl side chains (as opposed to cooperative backbone segmental motion or cross-linker chemistry), causing the $E_{a,\tau}$ of PHMA-B3-D2 to align with the $E_{a,\beta}^{\text{WLF}}$ of PHMA. With more static cross-links and less dynamic covalent cross-links, backbone segments will be less mobile during stress relaxation. In addition, with less dynamic covalent cross-links, cross-linker diffusion in order to reassociate with

- Acrolocular
Rapid Communications

www.mrc-journal.de

ported and calculated $E_{a,\alpha-\beta}$ ranges for PLMA, suggesting that, when percolated, static cross-links are present in the network architecture; the backbone and side chain motions associated with the alpha—beta relaxation process of PLMA facilitate and are necessary for large-scale stress relaxation. [108,109] Therefore, this process likely dictates the temperature dependence of stress relaxation in PLMA-B2-D3 instead of the BiTEMPS methacrylate cross-link dissociation or other mechanisms.

Finally, we note that the residual stress parameter $\sigma_{\rm perm}/\sigma_0$ is also useful in identifying the amount and role of permanent cross-links in the CANs. From Table 3, PHMA-B4-D1 with a lower density of permanent cross-links than PHMA-B3-D2, exhibited negligible residual stress ($\sigma_{\rm perm}/\sigma_0$ < 1%), characteristic of a number of permanent cross-links insufficient to achieve a percolated, permanent network. In contrast, PHMA-B3-D2 with a higher density of permanent cross-links exhibits much higher long-term residual stress (25–38% of σ_0), indicating sufficient permanent cross-link density to achieve a percolated, permanent network structure that can sustain stress at long times. Similarly for PLMA CANs, PLMA-B3-D2 exhibited very low residual stress ($\sigma_{\text{perm}}/\sigma_0$ between 2.1% and 5.5%) which was insufficient to affect (re)processability, high-T thermomechanical properties (such as the presence of a sustained, secondary rubbery plateau), or the temperature dependence of stress relaxation. On the other hand, PLMA-B2-D3 clearly possessed percolated, static cross-links in that it exhibited very high residual stress (σ_{perm}/σ_0) between 32% and 65%). This level of permanent cross-links was shown to have likely affected the initial processability of PLMA-B2-D3 into a 1st-molded film (as evidenced by a 20% drop between gel contents) as well as the temperature dependence of stress relaxation and high-T thermomechanical properties via DMA (through the presence of a sustained, secondary rubbery plateau up to 275 °C without reaching terminal flow).

new partners after an initial dissociation may become somewhat rate-limiting during stress relaxation and is likely weakened. The dissociation of BiTEMPS methacrylate cross-links in general may also be weakened as a result of the greater presence of static cross-links. One or more of these phenomena can cause n-hexyl side chains of PHMA-B3-D2 to become critical in facilitating the relaxation of stress which would explain the alignment of $E_{\rm a,r}$ for PHMA-B3-D2 and the $E_{\rm a,g}$ WLF for PHMA.

Given the relative ambiguity regarding the mechanisms responsible for stress relaxation in PHMA CANs containing both static and dynamic covalent cross-links, we seek greater clarity through investigations into another CAN system. Our PLMA CANs with static and dynamic covalent cross-links offer the opportunity to study these mechanisms further as PLMA has a vastly different activation energy for cooperative segmental relaxation than that of PHMA and, therefore, the BDEs of the sulfur-sulfur bonds of BiTEMPS methacrylate. [79,82-84,91,108,109] Polymethacrylates with side chains greater than ten carbons such as PLMA are not known to exhibit distinct alpha and beta relaxations but rather a coalesced alpha-beta relaxation.^[108] In the range of tested stress relaxation temperatures in this study (well above the T_g of PLMA), this coalesced alpha-beta relaxation has an activation energy $(E_{a,\alpha-\beta}^{\text{WLF}})$ that can be calculated using WLF parameters of 58–64 kJ mol⁻¹. [109] A second report on PLMA estimates its $E_{a,\alpha-\beta}$ to be 52–67 kJ mol⁻¹ above room temperature.^[108] If backbone and side chain motions are the driving forces behind stress relaxation of polymethacrylate CANs without static crosslinks then we would expect $E_{a,\tau}$ values for PLMA CANs without percolated, static cross-links to align with the reported $E_{a,\alpha-\beta}$ values for PLMA.

PLMA-B5, PLMA-B4-D1, and PLMA-B3-D2 are the three PLMA CANs without percolated, static cross-links. As seen in Figure 8, these CANs have $E_{a,\tau}$ values of 116 \pm 11 kJ mol⁻¹, $95 \pm 8 \text{ kJ mol}^{-1}$, and $115 \pm 4 \text{ kJ mol}^{-1}$, respectively; these values are either within experimental uncertainty or very close outside of experimental uncertainty of the BDEs of sulfur-sulfur bonds in BiTEMPS methacrylate. [79,82–84,91] These $E_{\mathrm{a},\tau}$ values also align strongly with those of PHMA CANs and other CANs containing BiTEMPS methacrylate cross-links such as polyethylene and ethylene/1-octene copolymer CANs. [15,85,87,88,90] Notably, these $E_{a,\tau}$ values are very different from reported and calculated $E_{a,\alpha-\beta}$ values for PLMA, indicating that the backbone and side chain motions associated with the alpha-beta relaxation process of PLMA are not responsible for the stress relaxation of these PLMA CANs.[108,109] Instead, our results lend credence to previous reports that the temperature dependence of stress relaxation of CANs containing BiTEMPS methacrylate cross-links (integrated into or grafted between CAN backbone chains) is governed by the mechanism by which BiTEMPS methacrylate cross-links dissociate and subsequently reassociate with other partners. $^{[15,85,87-89]}$ As the $E_{\rm a,\tau}$ values of the CANs without percolated, static cross-links align with the energies of dissociation (BDEs) of the sulfur-sulfur bonds of BiTEMPS methacrylate, the dissociation step of the dynamic covalent exchange mechanism is likely the rate-limiting step precluding stress relaxation.

As with PHMA-B3-D2 which contains percolated, static crosslinks, PLMA-B2-D3 exhibits a lower $E_{a,\tau}$ value (58 \pm 6 kJ mol⁻¹) than its other PLMA CAN counterparts without percolated, static cross-links. This $E_{a,\tau}$ is within experimental uncertainty of the re-

3. Conclusion

Using two sulfur-based cross-linkers with very different bond dissociation energies, we prepared several catalyst-free, polymethacrylate covalent adaptable networks (CANs) containing both static and dynamic covalent cross-links. We demonstrated the processability and recyclability of these networks with complete recovery of cross-link density and other thermomechanical properties. With judicious control of the cross-linker content, the formation of percolated, static cross-links can be attained without sacrificing (re)processability of our PHMA and PLMA CANs. In contrast, we also demonstrated that a catalyst-free network synthesized solely with static disulfide cross-links cannot be processed. Based on quantitative examinations of the stress relaxation responses of the CANs, we corroborated the presence of percolated, permanent cross-links, as such cross-links do not allow the complete relaxation of stresses. The stress relaxation results reported here also show that the incorporation of nonpercolated, static cross-links into CANs does not have any apparent effect on the T dependences ($E_{a,\tau}$ values) of their stress relaxation responses, as long as no percolated, permanent cross-links

The $E_{a,r}$ of our PHMA CAN with non-percolated, static crosslinks (PHMA-B4-D1) was 102 \pm 17 kJ mol⁻¹, which is within experimental uncertainty of the bond dissociation energies of





www.mrc-journal.de

the sulfur-sulfur bonds of BiTEMPS methacrylate (BDEs \approx 110– 130 kJ mol⁻¹),^[79,82-84] as well as of the activation energy of the alpha relaxation of neat PHMA ($E_{\rm a,\alpha}^{\rm WLF} \sim 97-105 \text{ kJ mol}^{-1}$).[107] In order to discern whether cross-link chemistry or cooperative segmental mobility is responsible for the stress relaxation behavior of PHMA-B4-D1, we subsequently studied the stress relaxation of our PLMA CANs, considering that neat PLMA has a very different activation energy associated with its cooperative segmental mobility than neat PHMA ($E_{\rm a,\alpha-\beta}^{\rm WLF} \sim 52\text{-}67 \text{ kJ mol}^{-1}$ for neat PLMA). We obtained $E_{\rm a,r}$ values of 116 \pm 11 kJ mol^{-1} , 95 \pm 8 kJ mol^{-1} , and 115 \pm 4 kJ mol^{-1} for our PLMA CANs containing no or small fractions of non-percolated, static cross-links. Thus, we argue that the temperature dependences of stress relaxation of our CANs with little to no non-percolated, static cross-links are governed by the dissociation of BiTEMPS methacrylate cross-links rather than by relaxations of backbone segments. Percolated, static cross-links strongly affected the dynamics and dominating mechanisms of stress relaxation in our CANs. Our PHMA and PLMA CANs containing percolated, static cross-links (PHMA-B3-D2 and PLMA-B2-D3) exhibited respective $E_{a,\tau}$ values of 56 \pm 7 kJ mol⁻¹ (which overlaps with the activation energy of the beta relaxation of neat PHMA, $E_{a,\beta}^{\rm WLF} \sim 54 \text{ kJ}$ mol⁻¹)^[107] and $58 \pm 6 \text{ kJ mol}^{-1}$ (which overlaps with $E_{a,\alpha-\beta}^{\rm WLF}$ of neat PLMA). This indicates that percolated, static cross-links resulted in the relaxations of *n*-hexyl side chains in PHMA CANs as well as of *n*-lauryl side chains and backbone segments in PLMA CANs to become critical in facilitating large-scale stress relaxation. Our study provides a simple approach to attain a better understanding of some of the viscoelastic behaviors of CANs that contain both static and dynamic covalent cross-links.

4. Experimental Section

Materials: All chemicals are commercially available and used as received unless otherwise noted. Bis (2-methacryloyl) oxyethyl disulfide (DS-DMA), petroleum ether (anhydrous), sulfur monochloride (S_2Cl_2 , 98%), *n*-hexyl methacrylate (HMA, 98%), *n*-lauryl methacrylate (LMA, 96%), azobisisobutyronitrile (AIBN, 98%), *N*,*N*-dimethylacetamide (DMAc, anhydrous, 99.8%), toluene (99.9%), and chloroform-*d* (CDCl₃, 99.8 atom% D) were from Sigma–Aldrich. 2,2,6,6-Tetramethyl-4-piperidyl methacrylate (TMPM) was purchased from TCI America. Dichloromethane (DCM, Certified ACS) and methanol (CH₃OH, 99.9%) were supplied by Fisher Scientific. HMA and LMA were de-inhibited using inhibitor remover (Sigma–Aldrich, 311340) in the presence of calcium hydride (Sigma–Aldrich, 90%). AIBN was recrystallized from CH₃OH. Petroleum ether and DMAc were dried over 4Å molecular sieves for at least 48 h before use.

Synthesis of BiTEMPS Methacrylate: Bis (2,2,6,6-tetramethyl-4-piperidyl methacrylate) n-sulfide (BiTEMPS methacrylate, n- = di, tri, tetra) was synthesized with the same procedure as compounds reported in refs. [15, 17, 86, 89, 90] (identified as BTMA in ref. [89] and as BTMA- S_n in ref. [90]). We note that the BiTEMPS methacrylate used in this study contains oligosulfide bridges of varying lengths, i.e., two, three, or four sulfurs. [90] As demonstrated in other studies, [90,91] oligosulfide analogues of BiTEMPS methacrylate have dynamic character and may be incorporated in a straightforward manner into robust and reprocessable CANs.

Synthesis of Dual Networks (PHMA-Bx-Dy and PLMA-Bx-Dy): In a typical synthesis, BiTEMPS methacrylate, DSDMA, and AIBN initiator were dissolved in HMA or LMA in a 20-mL glass vial using DMAc (~1.2 mL DMAc per g of HMA) as a solvent. BiTEMPS methacrylate and DSDMA cross-linkers were added in amounts such that the combined amount of cross-linkers in the networks totaled 5 mol%. Cross-linker mol%s were cal-

culated with respect to the total mols of HMA or LMA monomer and cross-linkers. In abbreviations used for CANs throughout this study (PHMA-Bx-Dy and PLMA-Bx-Dy), x and y represent the respective mol% of BiTEMPS methacrylate (B), the dynamic covalent cross-linker, and DSDMA (D), the static covalent cross-linker, used in the synthesis of the CAN. The concentration of the initiator, AlBN, was 1 mol% with respect to the total mols of monomer and cross-linkers. The reaction solutions were stirred at room temperature until homogenous mixtures were obtained. The solutions were subsequently bubbled with nitrogen (N2) gas at 70 °C for 15 min, after which N2 gas was allowed to flow continuously into the vial. The polymerizations proceeded at 70 °C for 24 h and were quenched by exposing them to air. The obtained networks were cut into small pieces, washed with DCM/CH3OH mixtures, and then dried in a vacuum oven at 80 °C for 24 h.

Using the same polymerization conditions as the dual networks, a permanently cross-linked PHMA network (PHMA-D5) was synthesized as a control sample using 5 mol% DSDMA cross-linker and 1 mol% AIBN, and a fully dynamic PLMA network (PLMA-B5) was synthesized using 5 mol% BiTEMPS methacrylate and 1 mol% AIBN. No BiTEMPS methacrylate was used in the synthesis of PHMA-D5, and no DSDMA was used in the synthesis of PLMA-B5. The networks were subsequently washed and dried in a similar manner to the dual networks.

Swelling: Swelling tests were performed by placing network samples in 20-mL glass vials filled with toluene. The samples were allowed to swell for at least 72 h, which is several days longer than the length of time needed to dissolve neat, entangled PHMA in toluene. [17,89] (Small sample pieces of neat, entangled PHMA and PLMA dissolved in toluene in less than 1 min.) Swollen samples were dried in a vacuum oven for at least 48 h to obtain gel fractions.

Differential Scanning Calorimetry (DSC): The glass transition temperatures ($T_{\rm g}$) of as-synthesized PHMA networks and melting temperatures ($T_{\rm m}$) of as-synthesized PLMA networks were obtained by DSC using a Mettler Toledo DSC822e. ~5-mg samples in hermetically sealed aluminum pans were heated to 80 °C at a rate of 20 °C min $^{-1}$ followed by cooling to -50 °C (for PHMA networks) or -80 °C (for PLMA networks) at the same rate. The samples were then heated to 80 °C at 10 °C min $^{-1}$. The $T_{\rm g}$ values of PHMA networks were obtained from the 2nd heating ramps using the 1/2 $\Delta C_{\rm p}$ method. $T_{\rm m}$ values of PLMA networks were determined from the endothermic peaks in the 2nd heating ramps. Percent crystallinities of the PLMA networks were estimated by integrating the endothermic peaks to obtain latent heats of fusion and calculating the ratios of these latent heats against the latent heat of fusion of n-alkanes in hexagonal packing (3.4 kJ mol $^{-1}$ per CH $_2$ unit, 37.4 kJ mol $^{-1}$ for fully crystalline PLMA containing 11 CH $_2$ units in each repeat unit). [92,93]

Thermogravimetric Analysis (TGA): Thermogravimetric analysis was performed using a Mettler Toledo TGA/DSC3+. The change in sample weight was recorded as a function of temperature upon heating samples under N_2 from 25 °C to 500 °C at a 10 °C min⁻¹ heating rate.

Molding and Reprocessing of Networks: (Re)processing of dried, assynthesized networks was done by hot pressing small network pieces into $\sim\!1\text{-mm-thick}$ sheets using a PHI press (Model 0230C-X1). (Re)processing was performed at 130 °C for 1 h using a 10-ton ram force. Unlike the dual networks, the permanently cross-linked PHMA network (PHMA-D5) could not be (re)processed into a healed film.

Dynamic Mechanical Analysis (DMA): Tension-mode DMA was performed using a TA Instruments RSA-G2 Solids Analyzer to characterize the thermomechanical properties of the network samples after each (re)processing step. In DMA experiments, tensile storage modulus (E'), tensile loss modulus (E''), and the damping ratio ($\tan \delta = E''/E'$) of the network samples were measured as functions of temperature. The network rectangular specimens were heated from 0 °C (for PHMA networks) to 150 °C or 300 °C at a heating rate of 3 °C min⁻¹. The measurements were collected at a frequency of 1 Hz and 0.03% oscillatory strain. At least two measurements were taken for each sample.

Stress Relaxation: Tensile stress relaxation measurements were performed on rectangular samples of the 1st-molded networks using a TA Instruments RSA-G2 Solids Analyzer. Samples were first annealed at the



www.mrc-journal.de

desired temperature for 10 min before a constant 5% tensile strain was applied.

Supporting Information

Supporting Information is available from the Wiley Online Library or from the author.

Acknowledgements

L.M.F. and M.A.B. contributed equally to this work. The authors acknowledge support provided by Leslie and Mac McQuown and the Center for Engineering Sustainability and Resilience (CESR) at the Northwestern University and by the National Science Foundation (NSF ECCS-1912694). The authors also acknowledge support from the Northwestern University via discretionary funds associated with a Walter P. Murphy Professorship (J.M.T.), from an NSF Graduate Research Fellowship (L.M.F.), and from SABIC (M.A.B.). This work made use of the MatCI Facility at Northwestern University, which receives support from the MRSEC Program (NSF DMR-1720139) of the Materials Research Center at Northwestern University.

Conflict of Interest

The authors declare no conflict of interest.

Author Contributions

L.M.F. did conceptualization, methodology, validation, formal analysis, investigation, data curation, visualization, writing – original draft, and writing – review and editing. M.A.B. did conceptualization, methodology, validation, formal analysis, investigation, data curation, visualization, writing – original draft, and writing – review & editing. C.C.O. did formal analysis, data curation, and investigation. M.A.G. did conceptualization, methodology, validation, funding acquisition, project administration, supervision, and writing – review & editing. J.M.T. did conceptualization, funding acquisition, validation, methodology, project administration, supervision, resources, and writing – review and editing.

Data Availability Statement

The data that support the findings of this study are available from the corresponding author upon reasonable request.

Keywords

covalent adaptable network, cross-link, dynamic, permanent, sustainability, vitrimer

Received: May 3, 2024 Revised: June 26, 2024 Published online:

- [1] E. Trovatti, T. M. Lacerda, A. J. F. Carvalho, A. Gandini, Adv. Mater. 2015, 27, 2242.
- [2] K. Jin, L. Li, J. M. Torkelson, Adv. Mater. 2016, 28, 6746.
- [3] W. Zou, J. Dong, Y. Luo, Q. Zhao, T. Xie, Adv. Mater. 2017, 29, 1606100

- [4] M. Röttger, T. Domenech, R. van der Weegen, A. Breuillac, R. Nicolaÿ, L. Leibler, Science 2017, 356, 62.
- [5] L. M. Polgar, M. van Duin, A. A. Broekhuis, F. Picchioni, Macromolecules 2015, 48, 7096.
- [6] C. J. Kloxin, T. F. Scott, B. J. Adzima, C. N. Bowman, *Macromolecules* 2010, 43, 2643.
- [7] M. Podgórski, B. D. Fairbanks, B. E. Kirkpatrick, M. McBride, A. Martinez, A. Dobson, N. J. Bongiardina, C. N. Bowman, Adv. Mater. 2020, 32, 1906876.
- [8] J. P. Kennedy, K. F. Castner, J. Polym. Sci., Polym. Chem. Ed. 1979, 17, 2039.
- [9] J. P. Kennedy, K. F. Castner, J. Polym. Sci., Polym. Chem. Ed. 1979, 17, 2055.
- [10] Z. Zhou, S. Chen, X. Xu, Y. Chen, L. Xu, Y. Zeng, F. Zhang, Prog. Org. Coat. 2021, 154, 106213.
- [11] X. Xu, S. Ma, S. Wang, J. Wu, Q. Li, N. Lu, Y. Liu, J. Yang, J. Feng, J. Zhu, J. Mater. Chem. A 2020, 8, 11261.
- [12] A. Ruiz de Luzuriaga, R. Martin, N. Markaide, A. Rekondo, G. Cabañero, J. Rodríguez, I. Odriozola, *Mater. Horiz.* 2016, 3, 241.
- [13] C. Lakatos, K. Czifrák, J. Karger-Kocsis, L. Daróczi, M. Zsuga, S. Kéki, J. Appl. Polym. Sci. 2016, 133, 44145.
- [14] J. J. Cash, T. Kubo, A. P. Bapat, B. S. Sumerlin, *Macromolecules* 2015, 48, 2098.
- [15] M. A. Bin Rusayyis, J. M. Torkelson, Polym. Chem. 2021, 12, 2760.
- [16] M. A. Bin Rusayyis, J. M. Torkelson, ACS Macro Lett. 2022, 11, 568.
- [17] M. Bin Rusayyis, J. M. Torkelson, Macromolecules 2020, 53, 8367.
- [18] Y. Amamoto, M. Kikuchi, H. Masunaga, S. Sasaki, H. Otsuka, A. Takahara, Macromolecules 2009, 42, 8733.
- [19] D. Montarnal, M. Capelot, F. Tournilhac, L. Leibler, Science 2011, 334, 965.
- [20] W. Denissen, G. Rivero, R. Nicolaÿ, L. Leibler, J. M. Winne, F. E. Du Prez, Adv. Funct. Mater. 2015, 25, 2451.
- [21] P. Cordier, F. Tournilhac, C. Soulié-Ziakovic, L. Leibler, Nature 2008, 451, 977
- [22] M. Capelot, M. M. Unterlass, F. Tournilhac, L. Leibler, ACS Macro Lett. 2012, 1, 789.
- [23] M. Capelot, D. Montarnal, F. Tournilhac, L. Leibler, J. Am. Chem. Soc. 2012, 134, 7664.
- [24] Y. Zhong, X. Wang, Z. Zheng, P. Du, J. Appl. Polym. Sci. 2015, 132,
- [25] Z. Xu, Y. Zhao, X. Wang, T. Lin, Chem. Commun. 2013, 49, 6755.
- [26] C. Shao, M. Wang, H. Chang, F. Xu, J. Yang, ACS Sustainable Chem. Eng. 2017, 5, 6167.
- [27] P. Du, M. Wu, X. Liu, Z. Zheng, X. Wang, T. Joncheray, Y. Zhang, J. Appl. Polym. Sci. 2014, 131, 40234.
- [28] P. Du, H. Jia, Q. Chen, Z. Zheng, X. Wang, D. Chen, J. Appl. Polym. Sci. 2016, 133, 43971.
- [29] C. E. Yuan, M. Z. Rong, M. Q. Zhang, Polymer 2014, 55, 1782.
- [30] H. Otsuka, K. Aotani, Y. Higaki, A. Takahara, J. Am. Chem. Soc. 2003, 125, 4064.
- [31] H. Otsuka, Polym. J. 2013, 45, 879.
- [32] T. Maeda, H. Otsuka, A. Takahara, Prog. Polym. Sci. 2009, 34, 581.
- [33] F. Caffy, R. Nicolaÿ, Polym. Chem. 2019, 10, 3107.
- [34] L. Li, X. Chen, K. Jin, M. Bin Rusayyis, J. M. Torkelson, *Macro-molecules* 2021, 54, 1452.
- [35] Z. Pei, Y. Yang, Q. Chen, Y. Wei, Y. Ji, Adv. Mater. 2016, 28, 156.
- [36] L. Li, X. Chen, K. Jin, J. M. Torkelson, Macromolecules 2018, 51, 5537.
- [37] M. M. Obadia, A. Jourdain, P. Cassagnau, D. Montarnal, E. Drockenmuller, Adv. Funct. Mater. 2017, 27, 1703258.
- [38] J. J. Lessard, L. F. Garcia, C. P. Easterling, M. B. Sims, K. C. Bentz, S. Arencibia, D. A. Savin, B. S. Sumerlin, *Macromolecules* 2019, 52, 2105.
- [39] W. Denissen, J. M. Winne, F. E. Du Prez, Chem. Sci. 2016, 7, 30.

272, 125858.



- [76] J. A. Yoon, J. Kamada, K. Koynov, J. Mohin, R. Nicolaÿ, Y. Zhang, A. C. Balazs, T. Kowalewski, K. Matyjaszewski, *Macromolecules* 2012, 45, 142.
- [41] L. Li, X. Chen, J. M. Torkelson, *Macromolecules* **2019**, *52*, 8207. 45, 142.
- [42] S. Hu, X. Chen, M. A. Bin Rusayyis, N. S. Purwanto, J. M. Torkelson, Polymer 2022, 252, 124971.

[40] N. S. Purwanto, Y. Chen, T. Wang, J. M. Torkelson, Polymer 2023,

- [43] X. Chen, L. Li, K. Jin, J. M. Torkelson, Polym. Chem. 2017, 8, 6349.
- [44] Y. Chen, B. Chen, J. M. Torkelson, Macromolecules 2023, 56, 3687.
- [45] L. Hammer, N. J. Van Zee, R. Nicolay, Polymers 2021, 13, 396.
- [46] Z. Yang, Q. Wang, T. Wang, ACS Appl. Mater. Interfaces 2016, 8, 21691.
- [47] Z. Q. Lei, H. P. Xiang, Y. J. Yuan, M. Z. Rong, M. Q. Zhang, Chem. Mater. 2014, 26, 2038.
- [48] W. Liu, D. F. Schmidt, E. Reynaud, Ind. Eng. Chem. Res. 2017, 56, 2667
- [49] L. H. Sperling, Introduction to Physical Polymer Science, John Wiley & Sons, Ltd., Hoboken, NJ 2006.
- [50] L. E. Nielsen, J. Macromol. Sci., Part C 1969, 3, 69.
- [51] D. J. Plazek, J. Polym. Sci., Part A-2: Polym. Phys. 1966, 4, 745.
- [52] K. Watanabe, Rubber Chem. Technol. 1962, 35, 182.
- [53] L. Chen, L. Zhang, P. J. Griffin, S. J. Rowan, *Macromol. Chem. Phys.* 2020, 221, 1900440.
- [54] J. J. Cash, T. Kubo, D. J. Dobbins, B. S. Sumerlin, *Polym. Chem.* 2018, 9, 2011.
- [55] A. Breuillac, A. Kassalias, R. Nicolay, Macromolecules 2019, 52, 7102.
- [56] Y. Spiesschaert, M. Guerre, I. De Baere, W. Van Paepegem, J. M. Winne, F. E. Du Prez, Macromolecules 2020, 53, 2485.
- [57] H. Zhang, C. Cai, W. Liu, D. Li, J. Zhang, N. Zhao, J. Xu, Sci. Rep. 2017, 7, 11833.
- [58] Y. Liu, Z. Tang, D. Wang, S. Wu, B. Guo, J. Mater. Chem. A 2019, 7, 26867.
- [59] L. Li, Doctoral Dissertation, Northwestern University 2019.
- [60] G. Lopez, L. Granado, G. Coquil, A. Lárez-Sosa, N. Louvain, B. Améduri, Macromolecules 2019, 52, 2148.
- [61] B. Zhang, Z. A. Digby, J. A. Flum, E. M. Foster, J. L. Sparks, D. Konkolewicz, *Polym. Chem.* 2015, 6, 7368.
- [62] Y. Zhou, R. Groote, J. G. P. Goossens, R. P. Sijbesma, J. P. A. Heuts, Polym. Chem. 2019, 10, 136.
- [63] M. O. Saed, A. Gablier, E. M. Terentejv, Adv. Funct. Mater. 2020, 30, 1906458.
- [64] Q. Li, S. Ma, S. Wang, Y. Liu, M. A. Taher, B. Wang, K. Huang, X. Xu, Y. Han, J. Zhu, Macromolecules 2020, 53, 1474.
- [65] Y. Yang, F.-S. Du, Z.-C. Li, Polym. Chem. 2020, 11, 1860.
- [66] C. A. Tretbar, J. A. Neal, Z. Guan, J. Am. Chem. Soc. 2019, 141, 16595.
- [67] H. Zhang, D. Wang, W. Liu, P. Li, J. Liu, C. Liu, J. Zhang, N. Zhao, J. Xu, J. Polym. Sci., Part A: Polym. Chem. 2017, 55, 2011.
- [68] P. Chakma, Z. A. Digby, J. Via, M. P. Shulman, J. L. Sparks, D. Konkolewicz, *Polym. Chem.* 2018, 9, 4744.
- [69] S. Wang, S. Ma, Q. Li, X. Xu, B. Wang, K. Huang, Y. liu, J. Zhu, Macro-molecules 2020, 53, 2919.
- [70] D. W. Hanzon, X. He, H. Yang, Q. Shi, K. Yu, Soft Matter 2017, 13, 7061
- [71] J. Ma, X. Mu, C. N. Bowman, Y. Sun, M. L. Dunn, H. J. Qi, D. Fang, J. Mech. Phys. Solids 2014, 70, 84.
- [72] Q. Li, S. Ma, N. Lu, J. Qiu, J. Ye, Y. Liu, S. Wang, Y. Han, B. Wang, X. Xu, Green Chem. 2020, 22, 7769.
- [73] S. Debnath, S. K. Tiwary, U. Ojha, ACS Appl. Polym. Mater. 2021, 3, 2166.
- [74] N. Lu, Q. Li, S. Ma, B. Wang, X. Xu, S. Wang, J. Ye, J. Qiu, J. Zhu, Eur. Polym. J. 2021, 147, 110291.
- [75] R. Nicolaÿ, J. Kamada, A. Van Wassen, K. Matyjaszewski, Macro-molecules 2010, 43, 4355.

- [77] S. Sunner, Acta Chem. Scand. 1955, 9, 837.
- [78] M. K. McBride, B. T. Worrell, T. Brown, L. M. Cox, N. Sowan, C. Wang, M. Podgorski, A. M. Martinez, C. N. Bowman, Annu. Rev. Chem. Biomol. Eng. 2019, 10, 175.
- [79] D. Sakamaki, S. Ghosh, S. Seki, Mater. Chem. Front. 2019, 3, 2270.
- [80] Y. H. Jo, S. Li, C. Zuo, Y. Zhang, H. Gan, S. Li, L. Yu, D. He, X. Xie, Z. Xue, Macromolecules 2020, 53, 1024.
- [81] A. Takahashi, R. Goseki, K. Ito, H. Otsuka, ACS Macro Lett. 2017, 6, 1280.
- [82] W. C. Danen, D. D. Newkirk, J. Am. Chem. Soc. 1976, 98, 516.
- [83] B. Maillard, K. U. Ingold, J. Am. Chem. Soc. 1976, 98, 520.
- [84] A. Takahashi, R. Goseki, H. Otsuka, Angew. Chem., Int. Ed. 2017, 56, 2016
- [85] L. M. Fenimore, B. Chen, J. M. Torkelson, J. Mater. Chem. A 2022, 10, 24726.
- [86] M. A. Bin Rusayyis, L. M. Fenimore, N. S. Purwanto, J. M. Torkelson, Polym. Chem. 2023, 14, 3519.
- [87] B. Chen, L. M. Fenimore, Y. Chen, S. M. Barbon, H. A. Brown, E. Auyeung, C. L. P. Shan, J. M. Torkelson, *Polym. Chem.* 2023, 14, 3621.
- [88] L. M. Fenimore, B. Chen, Y. Chen, S. M. Barbon, H. A. Brown, E. Auyeung, C. L. P. Shan, J. M. Torkelson, Eur. Polym. J. 2024, 202, 112661
- [89] L. M. Fenimore, M. J. Suazo, J. M. Torkelson, Macromolecules 2024, 57, 2756.
- [90] T. Debsharma, N. S. Purwanto, L. M. Fenimore, S. Mitchell, J. Kennedy, J. M. Torkelson, *Polym. Chem.* 2024, 15, 2167.
- [91] M. Aiba, T. Koizumi, M. Futamura, K. Okamoto, M. Yamanaka, Y. Ishigaki, M. Oda, C. Ooka, A. Tsuruoka, A. Takahashi, H. Otsuka, ACS Appl. Polym. Mater. 2020, 2, 4054.
- [92] G. W. H. Höhne, Polymer 2002, 43, 4689.
- [93] U. N. Arua, F. D. Blum, J. Polym. Sci., Part B: Polym. Phys. 2017, 56, 89
- [94] S. A. Greenberg, T. Alfrey, J. Am. Chem. Soc. 1954, 76, 6280.
- [95] P. J. Flory, Principles of Polymer Chemistry, Cornell University Press, Ithaca, NY 1953.
- [96] K. P. Menard, Dynamic Mechanical Analysis: A Practical Introduction, CRC Press, Bota Raton, FL 2008.
- [97] M. Aiba, T. Koizumi, K. Okamoto, M. Yamanaka, M. Futamura, Y. Ishigaki, M. Oda, C. Ooka, A. Takahashi, H. Otsuka, *Mater. Adv.* 2021, 2, 7709.
- [98] B. R. Elling, W. R. Dichtel, ACS Cent. Sci. 2020, 6, 1488.
- [99] V. Zhang, B. Kang, J. V. Accardo, J. A. Kalow, J. Am. Chem. Soc. 2022, 144, 22358.
- [100] J. C. Hooker, J. M. Torkelson, *Macromolecules* 1995, 28, 7683.
- [101] A. Dhinojwala, J. C. Hooker, J. M. Torkelson, J. Non-Cryst. Solids 1994, 172, 286.
- [102] R. Kohlrausch, Ann. Phys. 1847, 148, 353.
- [103] G. Williams, D. C. Watts, J. Chem. Soc. Faraday Trans. 1970, 66, 80.
- [104] M. Rubinstein, R. H. Colby, *Polymer Physics*, Oxford University Press, New York, NY 2003.
- [105] G. A. Parada, X. Zhao, Soft Matter 2018, 14, 5186.
- [106] R. G. Ricarte, S. Shanbhag, D. Ezzeddine, D. Barzycki, K. Fay, Macro-molecules 2023, 56, 6806.
- [107] W. C. Child, J. D. Ferry, J. Colloid Sci. 1957, 12, 389.
- [108] G. Williams, D. C. Watts, Trans. Faraday Soc. 1971, 67, 2793.
- [109] S. F. Kurath, T. P. Yin, J. W. Berge, J. D. Ferry, J. Colloid Sci. 1959, 14, 147.